Application and Analysis of Microbial Spray Filtering in Environmental Exhaust Gas Treatment

Yang Liao[ID], Yu Wang[*][ID], Shipeng Huang[ID]

School of Mechanical Engineering, Xihua University, 611730 Chengdu, China

[*] Correspondence: Yu Wang (wangyu@mail.xhu.edu.cn)

Citation: Y. Liao, Y. Wang, S. P. Huang, "Application and analysis of microbial spray filtering in environmental exhaust gas treatment," *Acadlore Trans. Geosci.*, vol. 1, no. 1, pp. 67-75, 2022. https://doi.org/10.56578/atg010108.

Abstract: Due to a number of circumstances, grain depots will emit exhaust gases that are harmful to the environment and the health of the surrounding population in addition to being complex in composition and challenging to manage. In order to cope with environmental exhaust gases, this work integrates microbial spray filtering with an exhaust gas treatment equipment. The authors ran simulations of the mixture of exhaust gases and the microbial solution using COMSOL Multiphysics at various pipe diameters, initial nozzle distances, nozzle number, and nozzle intervals. The findings indicate that the pipe diameter should be 300mm, the starting nozzle distance should be 290mm, there should be five nozzles, and the nozzle interval should be 200mm to obtain the optimal mixing of exhaust gases and the microbial solution. The study offers a useful guide for microbial deodorization.

Keywords: Organic exhaust gas; Spray filtering; Microbes; Numerical simulation

1. Introduction

Green grain storage methods have proliferated recently, including low-temperature storage [1, 2], controlled atmosphere storage [3], inert powder storage [4, 5], and recirculating fumigation storage [6, 7]. The quality of grain storage is superior thanks to this cutting-edge technology, but the expense to improve quality is higher. The majority of grain depots in China use traditional techniques of storage and chemical fumigation to eradicate insects [8]. At grain depots, chemical fumigation residue is a significant source of environmental exhaust gases that contain phosphide. A significant number of phosphides, a characteristic environmental exhaust gas, will be produced even during the strictest fumigation [9]. Sulfides and nitrides, two other sources of grain store exhaust gases, are produced by mildews when grains are exposed to air. These exhaust fumes will contaminate the environment and endanger people if they are released into the air directly.

Dry methods and wet methods are the two main categories for the many technical techniques used for domestic and international grain store exhaust gas degradation. Grain store exhaust gases can be immediately burned [10] by dry techniques or degraded [11] by using solid adsorbents or oxidants [12, 13]. Examples of such practices are the combustion method and the adsorption approach. The dry methods harm the environment despite their straightforward procedure and low cost. The liquid-phase oxidation reaction between exhaust gases and solutions containing oxidants or catalysts is primarily carried out using wet techniques. The plasma method [14, 15] and the biological method [16] are examples of wet methods. The plasma process has a broad variety of applications and a high rate of purification, but it also needs expensive equipment and uses a lot of energy. The biological approach uses straightforward, low-maintenance treatment equipment and has a high clearance efficiency. Additionally, it can prevent secondary contamination. The characteristics and applicability range of each exhaust gas removal technology are listed in Table 1.

The biological technique for exhaust gas treatment outperforms other conventional methods by a wide margin, as demonstrated in Table 1. Utilizing low-cost, straightforward, simple, easy-to-operate, manageable, and maintainable devices, the method can achieve effective treatment without any secondary contamination [17]. Microbial strains, meanwhile, have a lot of benefits. They can, for instance, adapt to a variety of harsh settings and

effectively treat exhaust gases. Almost every substance can be broken down by microorganisms. Microbes may grow on a variety of substrates and are both easily produced and self-replicating. Numerous exhaust gases can be treated with a relatively tiny number of microbial strains.

Table 1. Common malodorous gas treatment methods

Method	Technique	Applicable scope	Features
Combustion method	Degrading flammable malodorous substances through strong oxidation reaction	Suitable for treating flammable and malodorous substances with high concentration and small air volume.	Positive feature(s): High decomposition efficiency Negative feature(s): High probability of equipment corrosion, high fuel consumption, high cost, and possible generation of secondary pollutants during treatment
Oxidation method	Oxidizing malodorous substances with oxidant	Suitable for treating malodorous gases with medium to low concentration	Positive feature(s): High treatment efficiency Negative feature(s): Need for oxidant, and high treatment cost
Absorption method	Deodorizing gases by absorbing malodorous substances in the gases with solvent	Suitable for treating malodorous gases with medium to high concentration	Positive feature(s): Large treatment flow, and mature technology Negative feature(s): Low treatment efficiency, need for adsorbent, and pollutants merely transferred from the gas phase to the liquid phase
Adsorption method	Removing malodorous substances in malodorous gases with adsorbent	Suitable for treating malodorous gases with low concentration and high purification requirements	Positive feature(s): Capable of treating multi-component malodorous gases Negative feature(s): Low treatment efficiency
Plasma method	Promoting the reaction of exhaust pollutants with high-energy particle, converting the pollutants into carbon dioxide and water	Suitable for a wide range, and highly efficient in purification	Positive feature(s): Capable of treating multi-component malodorous gases that are not easily treated by other methods Negative feature(s): Expensive experiment, and high energy cost
Biological method	Deodorizing gases by degrading malodorous substances with microbes	Suitable for removing biodegradable water-soluble malodorous substances	Positive feature(s): High removal efficiency, simple treatment devices, low treatment cost, easy operation and maintenance, and capable of preventing secondary pollution

The theory behind the microbial treatment of grain storage exhaust gases is explained in this study. Microbial solution is first injected into the exhaust gas flow channel, followed by COMSOL Multiphysics simulation and optimization. The purpose is to optimize the exhaust gas treatment device, and improve the treatment efficiency.

2. Methodology

2.1 Principle of Exhaust Gas Treatment

Under the coexistence of water, microbes, and oxygen, exhaust gasses can be purified through the microbial metabolism, which oxides and decomposes the phosphides, sulfides, and nitrides in the gases. Microbial treatment can be roughly divided into the following three steps:

Step 1. The phosphides, sulfides, and nitrides are effectively exposed to the circulating biological bacteria liquid on the surface of the filler carrier, and fully dissolved in water.

Step 2. The microbes spread to the surface of the phosphides, sulfides, and nitrides dissolved in water, and absorb these substances.

Step 3. The microbes oxide and decompose the phosphides, sulfides, and nitrides. The phosphides are decomposed into PO_4^{-3}, the sulfides into S, $S_2O_3^{2-}$, and SO_4^{2-}, and the nitrides into NO_2^-, NH_4^-, and NO_3^-.

The specific mechanism is as follows:

Phosphides; Burkholderia cepacia (aerobic or anaerobic) [18]

Corynebacteria

Sulfides

Bacillus / Thiobacillus (aerobic or anaerobic) [19]

Photosynthetic bacteria (anaerobic, CO_2, and illumination)

Bacillus; Lactic acid bacteria; Saccharomycetes [20, 21]

Nitrides
Pseudomonas, etc.

2.2 Exhaust Gas Treatment Structure

According to the exhaust gas features, the appropriate working pH of the microbial solution is 4.0 ~ 6.0. Exhaust gases often contain acidic substances. When an exhaust gas in contact with microbial solution directly, the pH value of the solution will be reduced by these substances, which suppresses the efficiency of microbial treatment of the exhaust gas. For this reason, the acidic substances in the exhaust gas must be removed before the gas is in contact with the microbial solution. Then, the pH of the gas will be neutral, when it is exposed to the solution.

Figure 1 shows the principle of the exhaust gas treatment structure. The exhaust gas enters the pre-processing area for deacidification, such that the exhaust gas reaches the neutral state. Then, the near-neutral exhaust gas will reach the treatment area. To mix the microbial solution evenly with the exhaust gas, spray filtering will be adopted to spray the microbial solution into the exhaust gas pipe, using high-speed nozzles. It is an urgent problem to scientifically design the diameter of the exhaust gas pipe, and arrange the nozzles on that pipe.
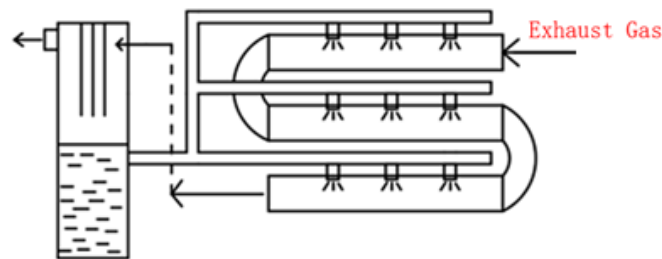

Figure 1. Principle of exhaust gas treatment structure

Based on COMSOL Multiphysics, a segment of exhaust gas treatment pipe was taken for numerical calculation to obtain the optimal pipe diameter and optimal nozzle distribution. The optimization results guide the design of pipe diameter and nozzle arrangement in actual production.

3. Simulation Analysis

3.1 Modeling

Compared with other simulation software, COMSOL Multiphysics, a simulation software package for multiple physical fields, has high degrees of freedom, and a convenient function input mechanism. The first half of the pipe where the exhaust gas first enters the mixing area was segmented for simulation. In this segment, the gas has just left from the pre-processing area, and features a high pressure and a fast speed. We simulated the nozzle distribution and the mixture between exhaust gas and microbial solution in this segment, which is more representative than other areas.
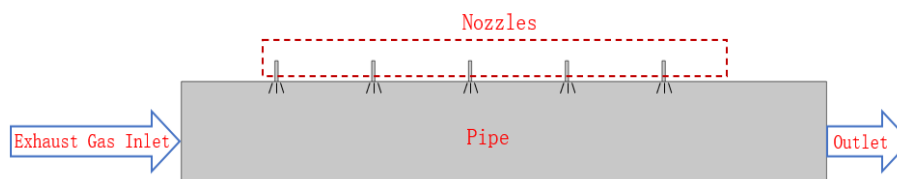

Figure 2. Spray filtering treatment model

Table 2. Initial values of parameterized coefficients

Parameter	Initial value	Name
L	2,000mm	Pipe length
D	300mm	Pipe diameter
a	190mm	Initial distance of nozzle
b	3	Number of nozzles
c	300mm	Nozzle interval

Given the symmetry of nozzles on the pipe, the pipe and nozzles were illustrated with a simple two-dimensional (2D) model to reduce the computing load. Figure 2 shows the situation of five nozzles arranged at an interval of 400mm. The factory mainly provides 300mm and 450mm pipe diameter; The initial distance of the nozzle cannot be too far away from the exhaust inlet, so 190mm is selected as the initial value; The number and spacing of nozzles should be considered in combination with pipe length and nozzle cost. The pipe length is 2000mm, and other parameters are parameterized, as shown in Table 2.

3.2 Boundary Conditions

Because the entire exhaust gas pipe is too long, the first half of the pipe where the exhaust gas first enters the mixing area was segmented for simulation. The inlet and outlet pressures of the segment were 1,100Pa and 1,000Pa, respectively. Considering the small pressure difference between the inlet a12314nd outlet, the exhaust gas in the segment was treated as incompressible. Given their complex compositions, the exhaust gas and microbial solution were respectively simplified as the air and water solution. The periodic velocity inlet was selected for nozzles. The velocity period is shown in Figure 3. The k-ε turbulence model of physical fields was couped with the horizontal set to simulate the exhaust gas transport, and the distribution of the microbial solution ejected by the nozzles. The mean density and mean viscosity were measured by the mean harmonic volume, and the mean harmonic mass, respectively. The time step was set to 0.05s, and the total time to 2s. The simulation considers the impact of gravity and surface tension on the results.
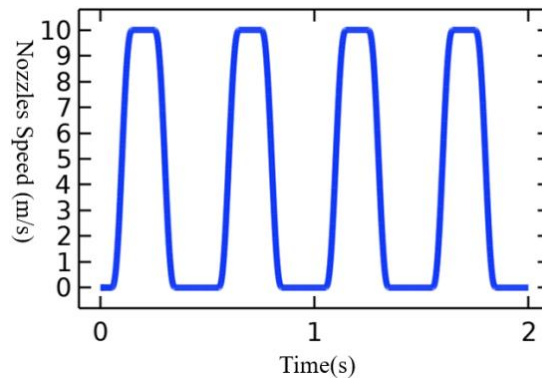

Figure 3. Ejection velocity period of microbial solution

3.3 Simulation Results

The simulations aim to disclose the impacts of two pipe diameters (300mm, and 450mm), four initial distances of nozzle (190mm, 290mm, 390mm, and 490mm), three different number of nozzles (3, 4, and 5), and four nozzle intervals (200mm, 300mm, 400mm, and 500mm).

3.3.1 Influence of pipe diameter on microbial solution distribution
Subgraph (a) and (b) of Figure 4 are the cloud maps for the velocity and microbial solution distribution at 0.4s, respectively, when the pipe diameter was 300mm, the initial distance of nozzle was 290mm, the number of nozzles was 4, and the nozzle interval was 400mm. Subgraph (c) and (d) of Figure 4 are the cloud maps for the velocity and microbial solution distribution at 0.4s, respectively, when the pipe diameter was 450mm, while all the other parameters remained the same.
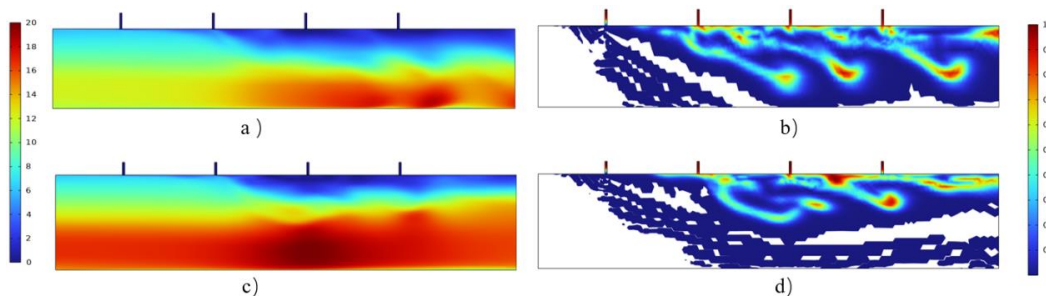

Figure 4. Influence of pipe diameter on microbial solution distribution

Comparing subgraph (c) of Figure 4 (pipe diameter: 450mm) with subgraph (a) of Figure 4 (pipe diameter: 300mm), it was observed that the velocity difference between the upper and lower layers in subgraph (c) of Figure 4 was more obvious than that in subgraph (a) of Figure 4. The velocity near the nozzles was much slower than that at the bottom of the pipe. Combined with the microbial solution distribution in subgraph (a) and (d) of Figure 4, it can be derived that the large difference between fast and low velocities disrupt the distribution of microbial solution.
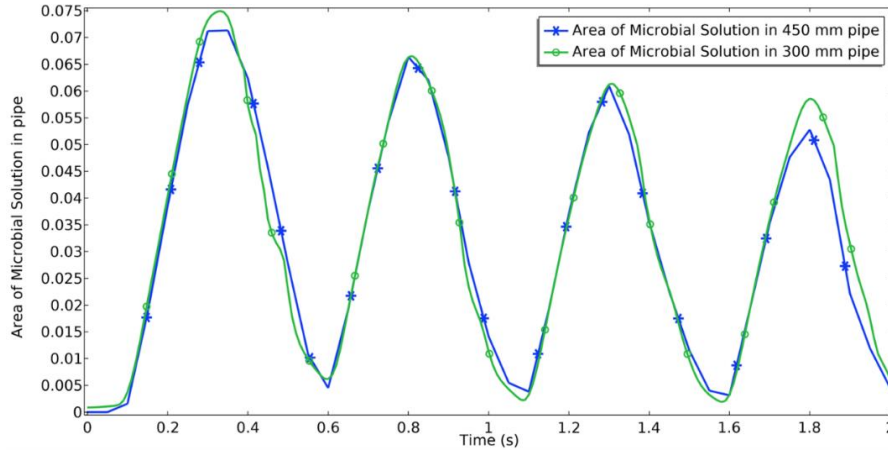

Figure 5. Volume fractions of the microbial solution with the two pipe diameters at different moments

Figure 5 shows the volume fractions of the microbial solution with the two pipe diameters at different moments. It can be observed that, under the periodic velocity inlet condition, the volume fraction of the microbial solution in the pipe slightly declined, after each velocity period. The decline was relatively small in the pipe with the smaller diameter. Thus, the small pipe diameter (300mm) is more favorable than the large pipe diameter (450mm).

3.3.2 Influence of initial distance of nozzle on microbial solution distribution

Figure 6 shows the simulation results at the pipe diameter of 300mm, with different initial distances of nozzles. The right subgraph shows the velocity distribution in the pipe at 0.4s, while the left subgraph shows the microbial solution distribution at 0.4s. The initial distance a_1 of the first nozzle was 190mm. Since the nozzle interval was 100mm, the initial distances b_1, c_1, and d_1 of the second, third, and fourth nozzles were 290mm, 390mm, and 490mm, respectively.

As shown in Figure 6, the closer the nozzle was to the exhaust gas inlet, the faster the velocity in the pipe, and the greater the difference between velocities in the upper and lower layers. Due to the velocity difference between the two layers, the microbial solution mainly concentrates in the upper part of the pipe. As a result, the microbial solution cannot fully mix with the exhaust gas, which suppresses the exhaust gas treatment effect.

When the nozzle was far from the exhaust gas inlet, e.g., d_1, the velocity difference between layers was greatly reduced, but the maximum velocity appeared at the middle of the pipe. Then, only the microbial solution from the first nozzle could easily reach the pipe bottom, while that from the other nozzles tend to concentrate in the upper part of the pipe.
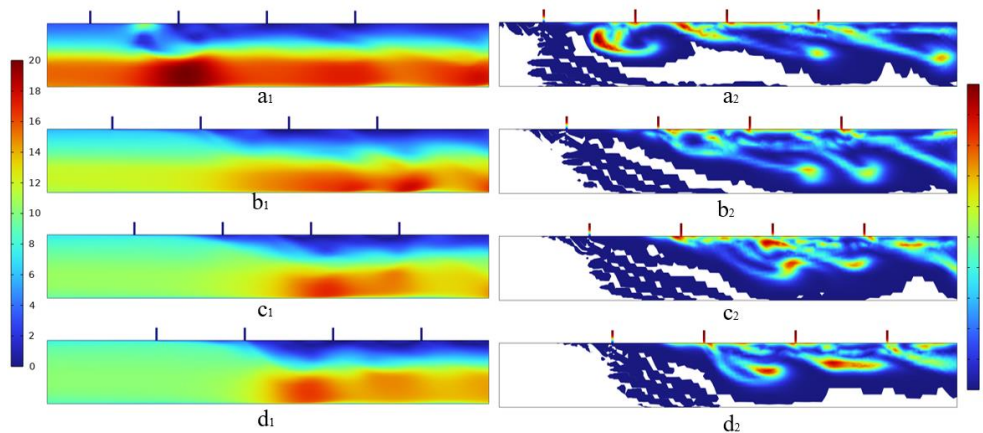

Figure 6. Influence of initial distance of nozzle on microbial solution distribution
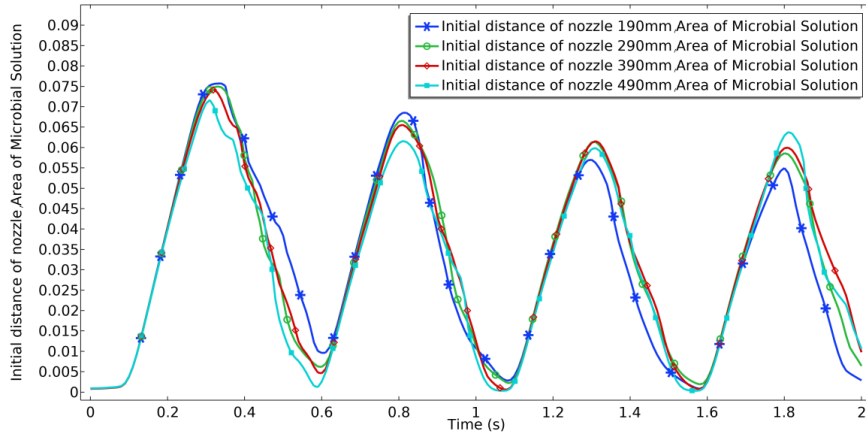
Figure 7. Volume fractions of the microbial solution with different initial distances of nozzle at different moments

When the nozzle was of moderate distance from the exhaust gas inlet, e.g., b_1 and c_1, the velocity difference between layers was much less significant than that of a_1, as evidenced by the velocity cloud maps. The cloud maps of microbial solution distribution also demonstrate that b_1 and c_1 are superior to d_1.

Figure 7 shows the volume fractions of the microbial solution with different initial distances of nozzle at different moments. It can be observed that, the volume fraction of the microbial solution in the pipe slightly declined, after each velocity period. When the initial distance of nozzle was 190mm, the volume fraction of the microbial solution was the highest initially, and the fastest in decline. When that distance was 490mm, the volume fraction of the microbial solution was the lowest initially, and the slowest in decline. Thus, neither distance is the optimal. There was an insignificant difference between the initial distances of 290mm and 390mm. With these two distances, the volume fractions of the microbial solution fell between those of the distance of 190mm and that of 490mm. Judging by the extremes of the volume fractions in Figure 7, the peak volume fraction at the distance of 290mm was higher than that at 390mm. Overall, the optimal initial distance of nozzle is 290mm.

3.4 Influence of Number of Nozzles on Microbial Solution Distribution

Figure 8 shows the simulation results with the pipe diameter of 300mm, the initial distance of nozzle of 290mm, nozzle interval of 400mm, and different number of nozzles. The right subgraph shows the velocity distribution in the pipe at 0.4s, while the left subgraph shows the microbial solution distribution at 0.4s. The number of nozzles a_1 was 3, b_1 was 4, and c_1 was 5.

As shown in Figure 8, with the growing number of nozzles, the velocity in the exhaust gas pipe became increasingly ununiform, and the microbial solution did not concentrate in the upper part of the pipe. By integrating the microbial solution in the pipe, the areas of microbial solution under a_1, b_1, and c_1 were determined as 0.0542 m^2, 0.0573 m^2, and 0.066 m^2, respectively. The 5 nozzle condition greatly improved the area from the 3 and 4 nozzle conditions. There was no significant difference between 3 and 4 nozzle conditions.

Figure 9 shows the volume fractions of the microbial solution with different number of nozzles at different moments. It can be observed that, the volume fraction of the microbial solution in the pipe slightly declined, after each velocity period. However, with the growing number of nozzles, the decline became smaller and smaller. Thus, more nozzles led to better performance. Five is clearly the optimal number of nozzles.
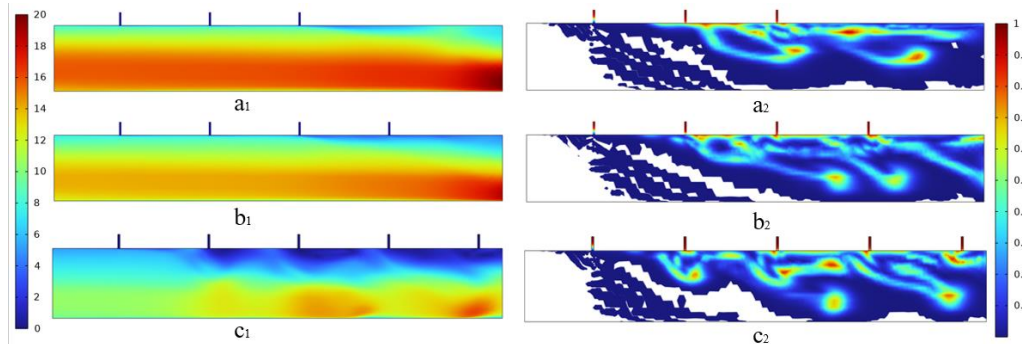

Figure 8. Influence of number of nozzles on microbial solution distribution
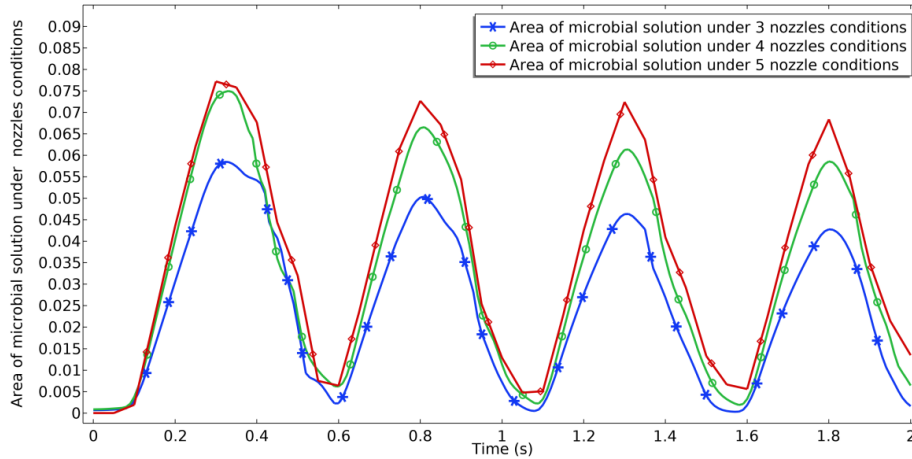
Figure 9. Volume fractions of the microbial solution with different number of nozzles at different moments

3.4.1 Influence of nozzle interval on microbial solution distribution

Figure 10 shows the simulation results with the pipe diameter of 300mm, the initial distance of nozzle of 290mm, number of nozzles of 5, and different nozzle intervals. The right subgraph shows the velocity distribution in the pipe at 0.4s, while the left subgraph shows the microbial solution distribution at 0.4s. The nozzle distance a_1 was 200mm, b_1 was 300mm, and c_1 was 400mm.

As shown in Figure 10, an obvious velocity difference was observed between the upper and lower parts of the pipe with a_1, b_1, and c_1. In the case of a_1, the peak velocity appeared at the back of the pipe; In the case of b_1, the peak velocity appeared at the middle of the pipe; In the case of c_1, the peak velocity appeared near the outlet.

According to the microbial solution distributions a_2, b_2, and c_2, the microbial solution was mixed well with the exhaust gas, always at the back of the pipe. By integrating the microbial solution in the pipe, the areas of microbial solution under a_2, b_2, and c_2 were determined as $0.0898 m^2$, $0.0802 m^2$, and $0.066 m^2$, respectively. Therefore, the best mixing between microbial solution and exhaust gas was realized at the nozzle interval of 200mm, followed by 300mm. The poorest mixing effect was observed at the nozzle interval of 400mm.
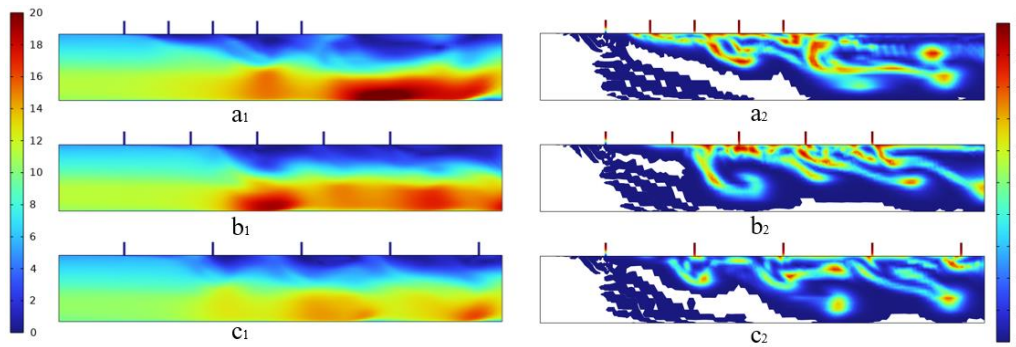

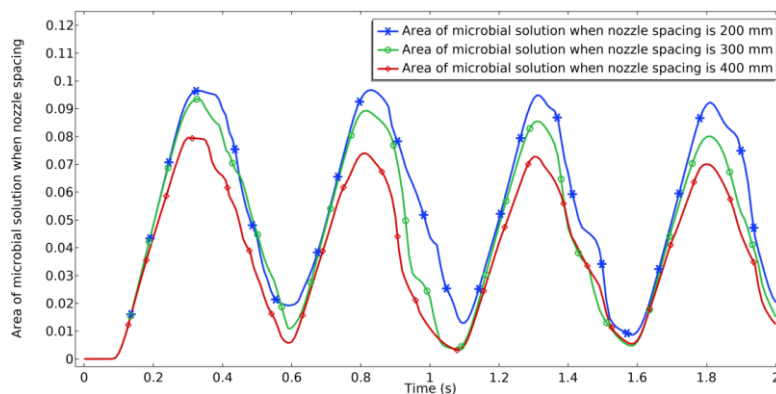**Figure 10.** Influence of nozzle interval on microbial solution distribution

Figure 11. Volume fractions of the microbial solution with different nozzle intervals at different moments

Figure 11 shows the volume fractions of the microbial solution with different nozzle intervals at different moments. It can be observed that, the volume fraction of the microbial solution in the pipe slightly declined, after each velocity period. When the nozzle interval was 200mm, the volume fraction decreased slowly, and remained at the highest possible level in all scenarios. Therefore, the smaller the nozzle interval, the better the mixing between the microbial solution and the exhaust gas. In other words, the nozzle interval of 200mm is better than 300mm and 400mm.

4. Conclusions

(1) Compared with the traditional way of exhaust gas treatment, microbial treatment of waste gas has obvious advantages, remarkable effect, no secondary pollution.

(2) Through numerical simulation, the influences of pipe diameter, initial distance of nozzles, number of nozzles, spacing of nozzles on the volume fraction of microbial solution in the pipe were analyzed, and the optimal distribution of nozzles was obtained. That is, when the diameter of the pipe is 300mm, the initial distance between the nozzles is 290mm, the number of nozzles is 5, and the distance between the nozzles is 200mm, the mixture of microbial solution and waste gas is the best, and the waste gas treatment effect is the best.

Data Availability

The data used to support the findings of this study are available from the corresponding author upon request.

Conflicts of Interest

The authors declare that they have no conflicts of interest.

References

[1] X. Y. Li, X. B. Xiong, Y. Zhang, S. Q. Wang, W. L. Jiang, and F. L. Xiu, "Effect of heat pipe-based low-temperature grain storage technology on wheat quality," *J. Chinese Cereals Oils Ass.*, vol. 30, no. 1, pp. 107-111, 2015. https://doi.org/10.3969/j.issn.1003-0174.2015.01.020.

[2] M. M. Ge, T. Ma, and J. H. Chen, "Green grain storage technology and its application effect analysis," *Grain Sci. Technol. Econ.*, vol. 44, no. 1, pp. 53-55, 2022. https://doi.org/10.16465/j.gste.cn 431252ts.20190113.

[3] M. Zhang and F. Y. Zhou, Food Storage, Beijing: Science Press, pp. 229-232, 2010.

[4] Z. J. Zhang, Y. Cao, J. Z. Li, J. Li, Y. Y. Li, Y. Wu, and Z. M. Wang, "Application of food-grade inert dust in grain store houses with inner circulation," *J. Henan U. Technol.* (*Nat. Sci. Edition*), vol. 5, pp. 103-107, 2019. https://doi.org/10.3969/j.issn.1673-2383.2019.03.019.

[5] I. Mewis and C. Ulrichs, "Action of amorphous diatomaceous earth against different stages of the stored product pests Tribolium confusum, Tenebrio molitor, Sitophilus granarius and Plodia interpunctella," *J. Stored. Prod. Res.*, vol. 37, no. 2, pp. 153-164, 2001. https://doi.org/10.1016/S0022-474X(00)00016-3.

[6] "Technical Specification for Phosphine Circulation Fumigation," LS/T 1201-2002, 2002.

[7] J. Xue, L. Zhou, L. Liu, and Y. Wu, "Control system of grain circulation fumigation based on agent," *Sci. J. Control. Eng.*, vol. 7, pp. 1-8, 2017.

[8] X. M. Gao and D. S. Lu, "Application practice of wheat green nitrogen for pest control and grain storage in tall and large scale warehouse," *Grain Proc.*, vol. 43, no. 5, pp. 78-80, 2018.

[9] D. Pan, T. J. Ma, K. Kang, and S. P. Bai, "Research progress on degradation technology of harmful gases in granary," *Food Machinery*, vol. 2020, no. 1, pp. 230-236, 2020. https://doi.org/10.13652/j.issn.1003-5788.2020.01.040.

[10] J. M. Colabella, R. A. Stall, and C. T. Sorenson, "The adsorption and subsequent oxidation of AsH3 and PH3 on activated carbon," *J. Cryst. Growth.*, vol. 92, no. 1-2, pp. 189-195, 1988. https://doi.org/10.1016/0022-0248(88)90449-6.

[11] S. C. Li, M. H. Liu, and Z. X. Pan, "Novel concentrated combustion method and its application in treatment of alcohol wastewater," *Environm. Engn.*, vol. 24, no. 6, pp. 73-73, 2006.

[12] Y. Xi, H. Yi, X. Tang, S. Zhao, Z. Yang, Y. Ma, T. Feng, and X. Cui, "Behaviors and kinetics of toluene adsorption-desorption on activated carbons with varying pore structure," *J. Environm. Sci.*, vol. 67, no. 5, pp. 104-114, 2018.

[13] D. Jecha, V. Brummer, P. Lestinsky, J. Martinec, and P. Stehlik, "Effective abatement of VOC and CO from acrylic acid and related production waste gas by catalytic oxidation," *Clean. Technol. Environm. Pol.*, vol. 16, no. 7, pp. 1329-1338, 2014. https://doi.org/10.1007/s10098-014-0750-7.

[14] S. K. Dai, W. Q. Xu, W. L. Tao, H. Qi, R. H. Liu, and T. Y. Zhu, "Experimental research for the application of O3 oxidation in simultaneous removal of SO₂, NO, and Hg in coal-fired flue gas," *Environ. Eng.*, vol. 10,

pp. 85-89, 2014. https://doi.org/10.1002/actp.1982.010330102.

[15] J. Q. Zhang, D. W. Yuan, X. Q. Zheng, S. X. Li, Q. Y. He, and W. G. Lv, "The application of electron beam radiation technology irradiation technology in the degradation of chemical contaminants," *Environm. Sci. Technol.*, vol. 2012, no. 3, pp. 75-78, 2012. https://doi.org/10.3969/j.issn.1674-4829.2012.03.021.

[16] E. C. Jeon, K. J. Kim, J. C. Kim, K. H. Kim, S. G. Chung, Y. Sunwoo, and Y. K. Park, "Novel hybrid technology for VOC control using an electron beam and catalyst," *Res. Chem. Intermed.*, vol. 34, no. 8, pp. 863-870, 2008. https://doi.org/10.1007/BF03036948.

[17] J. D. Wang, J. M. Chen, and X. Y. Tang, "Researches on organic waste gas treatment by biological methods," *Adv. Environm. Sci.*, vol. 6, no. 3, pp. 30-36, 1998.

[18] C. Y. Li, M. Chen, N. Sheng, Q. Liu, Z. H. Hu, M. Fang, and T. Zhang, "The characteristics and development of volatile organic compounds treatment technology," *Chem. Ind. Eng. P.*, vol. 2016, no. 3, pp. 917-925, 2016.

[19] X. B. Zhou, M. L. Chen, C. Y. Su, Z. Huang, H. J. Tang, and L. Y. Wang, "The influence mechanism of adsorption-biocoupling technology on phosphorus removal and microbial community analysis," *Technol. Water T.*, vol. 2022, no. 5, pp. 70-80, 2022.

[20] H. Shi, T. Y. Long, C. Liu, S. K. Wu, Y. Fan, and B. Liu, "Deep nitrogen removal from urban wastewater by ceramsite-sulfur mixed biological fillers based on heterotrophy-sulfur autotrophic denitrification coupling technology," *Chinese J. Environm. Eng.*, vol. 2022, no. 4, pp. 1363-1372, 2022.

[21] Y. L. Pan, "The application of three kinds of probiotics in recirculating aquaculture biofilter gifted," Ph.D. Dissertation, Ocean University of China, China, 2015.